

# Towards a comprehensive knowledge of the star cluster population in the Small Magellanic Cloud

A.E. Piatti<sup>1,2\*</sup>

<sup>1</sup>Consejo Nacional de Investigaciones Científicas y Técnicas, Av. Rivadavia 1917, C1033AAJ, Buenos Aires, Argentina

<sup>2</sup>Observatorio Astronómico, Universidad Nacional de Córdoba, Laprida 854, 5000, Córdoba, Argentina

Accepted XXX. Received YYY; in original form ZZZ

## ABSTRACT

The Small Magellanic Cloud (SMC) has recently been found to harbour more than two hundred per cent increase of its known cluster population. We provide here with solid evidence that such an unprecedented number of clusters could be largely over-estimated. On the one hand, the fully-automatic procedure used to identify such an enormous cluster candidate sample did not recover  $\sim 50$  per cent, in average, of the known relatively bright clusters located in the SMC main body. On the other hand, the number of new cluster candidates per time unit as a function of time results noticeably different to the intrinsic SMC cluster frequency (CF), which should not be the case if these new detections were genuine physical systems. We additionally found that the SMC CF varies spatially, in such a way that it resembles an outside-in process coupled with the effects of a relatively recent interaction with the Large Magellanic Cloud. By assuming that clusters and field stars share the same formation history, we showed for the first time that the cluster dissolution rate also depends on the position in the galaxy. The cluster dissolution results higher as the concentration of galaxy mass increases or external tidal forces are present.

**Key words:** techniques: photometric – galaxies: individual: SMC – galaxies: star clusters: general

## 1 INTRODUCTION

The number of star clusters identified in the Small Magellanic Cloud (SMC) has steadily grown from a handful of objects firstly recognised by [Shapley & Wilson \(1925\)](#) up to nearly six hundred clusters compiled in the catalogue of [Bica et al. \(2008, hereafter B08\)](#). Recently, [Bitsakis et al. \(2018, hereafter B18\)](#) reported a list of 1108 clusters that have not been reported before, distributed throughout the main body of the SMC. They searched for stellar overdensities on archival images of the Galaxy Evolution Explorer (GALEX/NUV, [Simons et al. 2014](#)), the Swift Ultraviolet-Optical Telescope (UVOT) Magellanic Clouds Survey (SUMAC, [Siegel et al. 2014](#)), the Magellanic Cloud Photometric Survey (MCPS, [Zaritsky et al. 2002](#)) and the “Surveying the Agents of a Galaxy’s Evolution SMC survey” (SAGE-SMC, [Gordon et al. 2011](#)), respectively. Then, they fitted theoretical isochrones from a Bayesian approach on field star cleaned colour-magnitude diagrams (CMDs) of the cluster candidates. The whole process - from the clus-

ter search until the age estimate - was fully-automatically carried out.

These new cluster candidates represent an increase of 215 per cent in the number of known clusters spread within the same areal coverage in the B08’s catalogue, which strikes our previous knowledge of the size of the SMC cluster population. Moreover, it is a bit of surprise that such a huge number of new objects have been detected from images that do reach in average comparable limiting magnitudes than those obtained by the Optical Gravitational Lensing Experiment (OGLE, [Pietrzynski et al. 1998](#)), which were used to perform the most recent update in the B08’s catalogue. Additionally, the spatial distribution of these new detections also differentiates from that coming from B08. The former is more broadly distributed in the sky, which contrasts with the elongated disc and bar shaped structures of the SMC main body.

In this paper we show that the compilation of clusters built by B18 would not seem representative of the SMC cluster population, so that by using it in statistical analyses could not lead to meaningful results. Our approach is threefold: in Section 2, we firstly conclude on the significant percentage of known relatively bright clusters that were not

\* E-mail: andres@oac.unc.edu.ar

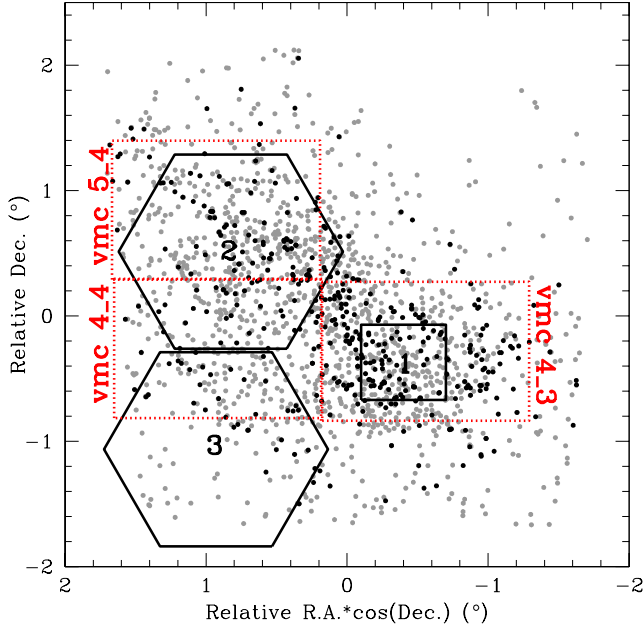


**Figure 1.** Spatial distribution of B18’s objects (grey dots) and those of Table 2 (black dots) with the SMC fields studied by Rubele et al. (2015) (red rectangles), Piatti et al. (2016) (black rectangle) and by Piatti (2017) (hexagons) overplotted.

included in B18. Then, we show that most of the new detections could not be related to relative faint still unidentified clusters. In Section 3, we finally show that the formation history of those new detections does not match that of the real SMC clusters. A summary of this work is presented in Section 4.

## 2 THE BULK OF THE SMC CLUSTER POPULATION

B18 matched their identified clusters with those in B08 for the same surveyed area, and found that only 211 out of 515 clusters were recovered at the end of their search-age estimate process. Their compilation represent  $\sim 40$  per cent of B08’s clusters. At a first glance, this seems a relatively low percentage of cluster recovery as to claim for accuracy and completeness in clusters detection. The matched clusters are included in their Table 1 with the running ID number used by B08. Unfortunately, they did not include the various cluster names more frequently used. As for the 1108 new detections, B18 simply did not find them in B08. However, after the cataloguing work by B08, more clusters have been identified and some few catalogued objects have been confirmed as possible non-physical systems throughout the B18’s covered area (see e.g., Glatt et al. 2010; Piatti & Bica 2012; Piatti et al. 2016).

We thus decided to build a catalogue as comprehensively as possible of SMC clusters distributed throughout the B18’s area with age estimates derived from isochrone fitting, in order to perform a thorough comparison with the B18’s one. For clusters younger than 1 Gyr, we used two major catalogues constructed by Chiosi et al. (2006) and Glatt

**Table 1.** Literature sources used to build the catalogue of SMC clusters with age estimates.

Reference	Data set	Number of clusters
Chiosi et al. (2006)	OGLE	122 (B08) + 112
Glatt et al. (2010)	MCPS	141 (B08) + 153
Maia et al. (2014)	Washington	29 (B08)
Piatti et al. (2007)	Washington	5 (B08)
Piatti et al. (2008)	Washington	7 (B08)
Piatti (2011a)	Washington	6 (B08)
Piatti (2011b)	Washington	9 (B08)
Piatti & Bica (2012)	Washington	3 (B08)

**Table 2.** Age estimates of SMC clusters<sup>a</sup>

Cluster name	log(age)	$\sigma(\log(\text{age}))$	n
–	–	–	–
B55,SOGLE60	8.15	0.18	3
B54,SOGLE62	8.20	0.10	2
H86-106w	8.67	0.03	2
–	–	–	–

<sup>a</sup> A portion of the table is presented here for guidance of its contents. The entire table is available as Supplementary material in the online version of the journal.

et al. (2010). This age cut off was imposed because of the very well-known limiting magnitude of the photometric data sets used by them, i.e. OGLE and MCPS, respectively (see figure 3 in B18). We complemented this gathering with ages derived by Piatti et al. (2007, 2008) and Maia et al. (2014) from slightly deeper Washington photometry. For older clusters, we used a series of works based on Washington photometry (Piatti 2011b,a). Whenever more than one age estimate is available, we averaged all values. Table 1 shows the different literature sources that contribute to the resulting catalogue - distinguishing the number of clusters found in B08 -, while the resulting list of the 419 clusters with the compiled averaged ages, their respective standard dispersion and the number of age values used are included in Table 2. The B08’s catalogue also comprises 139 clusters without age estimates, so that our compilation of ages represents  $\sim 75$  per cent of the total number of clusters included in B08, Chiosi et al. (2006) and Glatt et al. (2010), located within the B18’s area. Fig. 1 shows the spatial distributions of B18’s objects and those of Table 2, for comparison purposes.

We then cross-correlated the B18’s list of clusters with that of B08 on the basis of their coordinates using the IRAF<sup>1</sup>.TMATCH task. It provides two tables that include matched and unmatched objects, respectively, within a certain tolerance distance. We started with a distance of 0.60 arcmin to avoid multiple matchings. From the unmatched objects, we run again TMATCH for a distance of 0.85 arcmin, and iterated the procedure from the resulting unmatched sample for a distance of 1.00 arcmin. None execution of TMATCH produced multiple matchings. We thus

<sup>1</sup> IRAF is distributed by the National Optical Astronomy Observatories, which is operated by the Association of Universities for Research in Astronomy, Inc., under contract with the National Science Foundation.

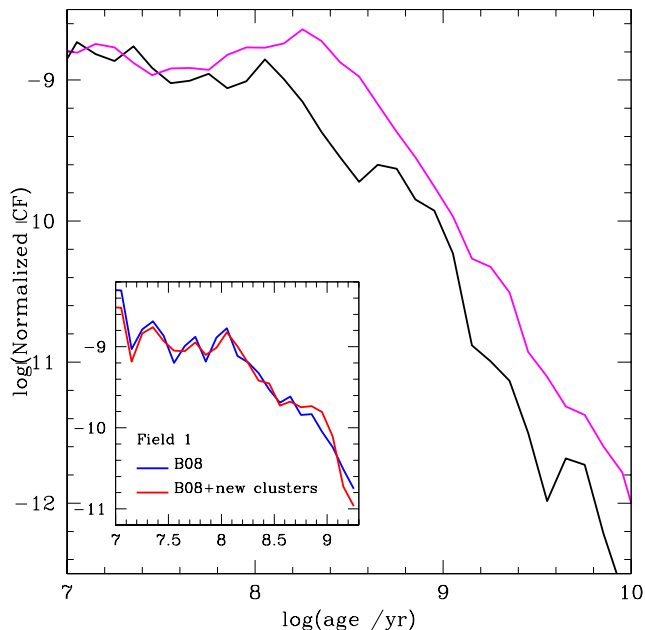


**Figure 2.** CFs for SMC clusters and B18’s new detections drawn with black and magenta lines, respectively. The inset panel depicts the CFs for two different cluster samples in Field 1 (see also Fig. 1).

found a total of 159 clusters cross-identified. Note that we performed the matching in a relatively relaxed fashion, because the tolerance distances employed are bigger than the smallest SMC clusters, which are typically of  $\sim 0.15$ - $0.20$  arcmin wide in radius (Piatti et al. 2016). Other additional 52 clusters were cross-correlated using distances between 1.00 and 4.00 arcmin. The matching of B18’s compilation with Chiosi et al. (2006)’s and Glatt et al. (2010) produced 11 (5%) and 60 (20%) identifications, respectively, which are very low numbers compared with those of other automatic cluster searching techniques (Pietrzyński et al. 1998; Ivanov et al. 2017, and references therein). These outcomes reveal that the B18’s compilation of SMC clusters is not statistically complete (see also Section 3).

Despite many relatively bright aggregates are not included in B18’s Table 1, their new detections could be faint clusters, though. In order to probe this possibility, we took advantage of two recent results on search of new SMC clusters. Piatti et al. (2016) used the VISTA<sup>2</sup> near-infrared  $YJK_s$  Magellanic Clouds survey data sets (VMC, Cioni et al. 2011) to explore a  $36' \times 36'$  region centred on the South-west of the SMC bar (Field 1 in Table 3 and Fig. 1). The area is one of the most crowded and highly affected by interstellar reddening in the galaxy, so that hidden clusters could exist there. They surveyed that region looking for clusters with dimensions and mean stellar densities in the same ranges than those previously known from optical passband photometric studies. They finally found 38 bona fide clusters, which represent an increase of  $\sim 55$  per cent in the number of known clusters in that area. On the other hand,

**Table 3.** Statistics of clusters in SMC fields.

Field ID	B08	New clusters	Ref.	B18’s objects		
				B08	New clusters	New detections
1	68	38	1	29	6	81
2	113	3	2	63	0	308
3	34	3	2	14	0	110

Ref.: (1) Piatti et al. (2016); (2) Piatti (2017).

Piatti (2017) employed an upgraded version of the cluster searching technique developed by Piatti et al. (2016) to seek new clusters in a vast area of the SMC (Fields 2 and 3 in Table 3 and Fig. 1). He made use of deep images from the Magellanic Stellar History (SMASH) survey and found very few new cluster candidates. Fig. 1 illustrates the position of the aforementioned fields.

We applied the TMATCH routine to cross-correlate the B18’s catalogue with those built by Piatti et al. (2016) and Piatti (2017), respectively, following the recipe described above. We started with a tolerance distance of 0.60 arcmin and increased it in steps of 0.15 arcmin up to 1.00 arcmin; no multiple cross-correlations were produced. The results are shown in Table 3, where we successively listed for Fields 1, 2 and 3 the number of clusters already included in B08 and those recently discovered by Piatti et al. (2016) and Piatti (2017), for comparison purposes. The total number of B18’s objects has been split in three columns, namely: B08’s clusters, Piatti et al. (2016)’s and Piatti (2017)’s new clusters, and B18’s new detections. As can be seen, when comparing the different catalogues with that of B18, we confirm the relatively high percentage of unmatched B08’s clusters, that goes from 44 per cent up to 59 per cent, with an average of 53 per cent. Unfortunately, a similar conclusion is drawn for recently discovered clusters; the number of new detections remaining notably high as well. As far as we are aware, the latter would not appear to be related to genuine physical systems. Since B18’s catalogue contains  $\sim 84$  per cent of them, their interpretations of the SMC cluster formation history and that of SMC-LMC interaction should be considered with caution.

### 3 THE SMC CLUSTER FREQUENCY

Beside the statistics of clusters that provided us with a strong evidence on the content of the B18’s list of objects, the ages derived by them also play an important independent role in describing their characteristics. These age estimates tell us about the formation history of the catalogued objects, so that in case they were real clusters, they should reproduce the formation history of the SMC cluster population. Otherwise, the formation history constructed from their assigned ages will differ from that one.

<sup>2</sup> Infrared Survey Telescope for Astronomy

It has been shown that the so-called cluster frequency (CF) is a more appropriate tool to describe the cluster formation history than the age histograms (see, e.g., Baumgardt et al. 2013; Piatti 2014; Piskunov et al. 2018). The former traces the number of clusters per time unit, while histogram bins could span different time interval. For instance, a histogram in  $\log(\text{age})$  with bin sizes of 0.1 embraces periods of time of  $\sim 2.6$  Myr and  $\sim 260$  Myr at the age intervals of  $\log(\text{age}) = 7.0-7.1$  and  $9.0-9.1$ , respectively. This uneven split of the whole time period could produce spurious peaks in the number of clusters at certain age bins, thus misleading the interpretation about enhanced periods of cluster formation, periods of more intense cluster dissolution, etc., among others. Particularly, the analysis of the SMC cluster formation history and the interaction with the LMC carried out B18 relies on age histograms.

In order to build the SMC CF we considered each age estimate of Table 2 as represented by an one-dimensional *Gaussian* of unity area centred at the respective age value, with a FWHM/2 equals to the age error. Then, we used a grid of age bins with sizes of  $\Delta(\log(\text{age})) = 0.1$  and added the fractions of the *Gaussians'* areas that fall into the bin boundaries. For instance, a point that is centred at any age interval and has an error smaller than  $\Delta(\log(\text{age})) = 0.05$  contributes with an amount of 1.0 to the total number of clusters to that age bin. Thus, by taking into account the uncertainties of the age estimates, we were able to produce an intrinsic SMC cluster age distribution. We then divided the total number of clusters per age bin by the size of the respective interval to obtain the corresponding CF. Fig. 2 shows the resulting CF drawn with a solid black line, normalised to the total number of clusters for comparison purposes.

Although it has been built with  $\sim 75$  per cent of all the catalogued clusters located within the B18's area, it results statistically representative of the whole SMC cluster population in that region. Indeed, Maschberger & Kroupa (2011) and Piatti (2014) have shown that cut-offs of the low-mass cluster regime (cluster mass  $\lesssim 10^3 M_{\odot}$ ) does not impact in the shape of the resulting CF. With a mass cut-off at  $5 \times 10^3 M_{\odot}$ , accurate CFs are still feasible to obtain. Nevertheless, for the sake of the reader we separately built the CFs for clusters located in Field 1, using the previously known 68 ones (B08) and the new discovered 38 clusters by Piatti et al. (2016) (see Table 3), respectively. The inset panel of Fig. 2 presents both resulting CFs. As can be seen, the new relatively faint clusters are imprinted with the same formation history than the most massive ones. Therefore, if the B18's new detections were faint genuine clusters, their CF should look like the one we built for the SMC. However, by following the same procedure described above to build the SMC CF, we constructed that from the B18's new detections, which resulted remarkably different to the former, as judged by the magenta solid line drawn in Fig. 2. Nevertheless, the B18's sample does not include relatively faint objects, because of the limiting magnitude of the photometric data sets used (see discussion in Section 2).

### 3.1 Cluster dissolution across the SMC

The CF constructed from clusters compiled in Table 2 represent the overall present-day distribution of the SMC cluster population as a function of age. However, such a distribution

could vary with the position in the galaxy. For instance, Piatti (2014) used the Harris & Zaritsky (2009)'s LMC regions to show that there exist some variations of the CFs from one region to another: 30 Doradus is the region with the highest relative CF for the youngest clusters, while the inner LMC regions have larger numbers of clusters during the period 1-3 Gyr than the outer ones. On the other hand, Baumgardt et al. (2013) showed that the LMC cluster dissolution has played a role for clusters older than 200 Myr. By adopting the star formation rate (SFR) derived by Harris & Zaritsky (2009) as the cluster formation rate (CFR), they found that about 90 per cent of them are lost per dex of lifetime. Therefore, in general, the present-day CF could result in a complex function which depends on both the local CFR and the cluster disruption.

Rubele et al. (2015) made use of the VMC database to build the SMC SFR producing not only an overall SFR for the whole galaxy, but also local SFRs for homogeneously distributed regions of  $\sim 22' \times 22'$  (see their figure 5). Three VMC tiles span over the SMC main body as illustrated in Fig. 1, so that we take advantage here of the respective SFRs. Rubele et al. (2015) split each tile in twelve sub-fields: four columns along the Right Ascension axis and three rows along the Declination axis. The sub-fields, from #1 to #12 were allocated across each tile from the bottom-left corner to the top-right one, i.e., by decreasing Right Ascension and increasing Declination. We used those SFRs to build CFs by adopting a power-law cluster mass distribution with a slope  $\alpha = -2$  and assuming that clusters and field stars share the same formation rates (SFR  $\equiv$  CFR). CFs and CFRs are linked through the expression:

$$CF_{SFR} = SFR \times \frac{\sum m^{-2}}{\sum m^{-1}} \quad (1)$$

where  $m$  is the cluster mass and the sums are computed over the SMC cluster mass range. Additionally, we constructed CFs for each sub-field from our compilation of clusters with age estimates (Table 2) following the same recipe employed above, i.e., by considering each age value as a *Gaussian* of unity area and adding the contribution of each *Gaussian* to different age intervals. The resulting present-day sub-fields CFs are depicted in Fig. 3.

A close inspection of Fig. 3 reveals that the cluster formation has not been continuous, but a process with relative short and long periods that has varied with the position in the galaxy. At the same time, it is possible to connect sub-fields that have experienced cluster formation at the same time, namely: 1) relatively old formation episodes in the outermost Western sub-fields (VMC 4.3.8 and 4.3.12); 2) no recent ( $\log(\text{age}) < 8$ ) cluster formation in outer sub-fields (VMC 5.4.9, 5.4.10, 5.4.11, 5.4.12, 4.4.2, 4.4.3, 4.4.4 and 4.3.11) and; 3) intense cluster formation in the SMC bar (VMC 5.4.3, 5.4.4, 4.4.12, 4.3.1, 4.3.2, 4.3.5, 4.3.6, 4.3.9). All these features are compatible with an outside-in formation process (see, e.g. Noël et al. 2009; Sabbi et al. 2009; Weisz et al. 2013). On the other hand, isolated relatively short cluster enhancements are seen towards the outermost Eastern sub-fields (VMC 4.4.1, 4.4.5, and 4.4.9), which could be part of the onset of the Magellanic bridge where recent field star and cluster formation took place (Piatti et al. 2015; Bica et al. 2015; Mackey et al. 2017).



**Table 4.** Fitted coefficients for the CF/CF<sub>SFR</sub> relationship.

Field	VMC 4_3				VMC 4_4				VMC 5_4			
	zero point	linear term	rms	$\chi^2$	zero point	linear term	rms	$\chi^2$	zero point	linear term	rms	$\chi^2$
1	9.30 ± 0.71	-1.17 ± 0.06	0.12	0.018	8.10 ± 1.40	-1.01 ± 0.16	0.17	0.035	—	—	—	—
2	10.28 ± 0.51	-1.29 ± 0.06	0.07	0.006	6.20 ± 0.97	-0.76 ± 0.10	0.12	0.018	3.62 ± 0.61	-0.48 ± 0.07	0.04	0.002
3	10.55 ± 0.62	-1.35 ± 0.07	0.05	0.003	7.13 ± 1.53	-0.93 ± 0.17	0.26	0.075	7.03 ± 1.45	-0.92 ± 0.17	0.24	0.065
4	7.45 ± 2.77	-0.94 ± 0.31	0.22	0.060	5.17 ± 1.01	-0.64 ± 0.11	0.07	0.005	6.90 ± 1.54	-0.90 ± 0.18	0.15	0.027
5	12.18 ± 1.11	-1.51 ± 0.13	0.12	0.018	10.21 ± 1.00	-1.22 ± 0.19	0.24	0.050	—	—	—	—
6	8.00 ± 1.00	-1.00 ± 0.11	0.17	0.032	10.42 ± 0.95	-1.31 ± 0.11	0.25	0.070	5.27 ± 0.59	-0.75 ± 0.07	0.18	0.036
7	4.81 ± 0.42	-0.62 ± 0.04	0.08	0.008	9.56 ± 1.64	-1.20 ± 0.19	0.16	0.031	5.19 ± 0.49	-0.72 ± 0.06	0.16	0.028
8	10.96 ± 1.27	-1.32 ± 0.14	0.10	0.012	9.23 ± 0.94	-1.15 ± 0.10	0.14	0.024	6.27 ± 0.94	-0.82 ± 0.11	0.13	0.021
9	6.28 ± 1.28	-0.86 ± 0.15	0.27	0.080	—	—	—	—	5.00 ± 0.86	-0.62 ± 0.10	0.09	0.010
10	12.21 ± 1.83	-1.49 ± 0.21	0.15	0.026	8.92 ± 1.59	-1.11 ± 0.14	0.18	0.039	6.48 ± 1.48	-0.80 ± 0.17	0.10	0.013
11	9.80 ± 3.36	-1.20 ± 0.39	0.09	0.013	7.86 ± 0.54	-1.00 ± 0.06	0.12	0.016	6.12 ± 1.78	-0.77 ± 0.23	0.12	0.019
12	8.50 ± 3.90	-1.00 ± 0.44	0.12	0.020	10.89 ± 1.65	-1.39 ± 0.19	0.19	0.041	—	—	—	—

We divided the present-day sub-field CFs by the respective CF<sub>SFR</sub> obtained from eq. (1) in order to find out any hint of dissolution. The results are presented in Fig. 4. Similarly to Baumgardt et al. (2013)’s outcomes, the number of observed clusters and those estimated from the Rubele et al. (2015)’s SFR are comparable for ages younger than  $\log(\text{age}) \sim 7.8 - 8.2$ , depending on the position in the galaxy. For older ages, the number of observed clusters clearly turn to decrease as a consequence of their dissolution with time. We fitted linear relationships of the CF/CF<sub>SFR</sub> ratios as a function of  $\log(\text{age})$  for the period where cluster dissolution is detected. The resulting coefficients are shown in Table 4, while Fig. 4 illustrates the derived linear relationships.

As can be seen, the slope - which is a measure of the dissolution rate - changes with the position in the galaxy. In order to highlight such a variation, we produced Fig. 5, which shows the spatial distribution of SMC clusters with green dots and grey-scale filled circles placed at the centre of the VMC sub-fields representing the respective CF/CF<sub>SFR</sub> slope values. Sub-fields in the Northern part of the SMC main body ( $\Delta(\text{Dec.}) > 0.5^\circ$ ) seem to share similar relatively low disruption rates, while those of the innermost part of the SMC, as well as those at the onset of the Magellanic bridge, have higher rates of dissolution. Since cluster disruption is mainly caused by the SMC tidal field, we speculate with the possibility that these findings confirm that clusters located in more massive galactic regions suffer more pronounced tidal effects. In addition, the relative large CF/CF<sub>SFR</sub> slope values for sub-fields located towards the South-East could be caused by the interaction with the LMC, which has been detaching the SMC gas and stellar content along the Magellanic bridge (Skowron et al. 2014; Noël et al. 2015; Carrera et al. 2017). Notice that if the cluster formation were not assumed to be that of the respective star field, the results of Fig. 5 would reveal that the CFR could differ significantly with respect to the SFR with position in the galaxy.

#### 4 CONCLUSIONS

In this study we addressed the issue of the unexpected large number of new cluster candidates compiled by B18. These

candidates represent more than two hundred per cent increase of the known SMC cluster population

We showed that the fully-automatic procedure implemented by B18 to detect and derive age estimates of cluster candidates did not completely recover the previously known bright catalogued clusters, neither those relatively faint ones recently discovered. To arrive to such a conclusion, we thoroughly searched the literature in order to compile a list of clusters as comprehensive as possible, including those listed in major cataloguing works and those from most recent cluster searches in particular SMC regions. We then used a proven technique that reliably cross-identified each object in the B18’s catalogue to its most probable counterpart in our own compilation and found that, in average, more than 50 per cent of the known clusters located in the SMC main body are not included in B18. Notably, a huge amount of B18’s new detections remained unmatched.

Nearly 75 per cent of all catalogued clusters have previous age estimates based on isochrone fitting to the cluster CMDs. After averaging the individual age values found in the literature, we constructed their global CF, which represents the intrinsic distribution of SMC clusters per time unit as a function of time. To build such a CF, we took into account the age uncertainties, so that the resulting distribution does not depend on the chosen age bins. Likewise, we showed that its shape would not vary if we used the entire SMC cluster population. We also produced a CF for the B18’s new detections ( $\sim 84$  per cent of their whole sample) and found that it turned out to be noticeably different from the SMC CF. Hence, we concluded that the B18’s catalogued could be contaminated with non-cluster objects.

We finally analysed the dependence of the CF with the position in the galaxy. In order to do that, we built CFs for regions of  $\sim 0.13$  square degrees homogeneously distributed across the SMC main body. The resulting CFs confirm the outside-in cluster formation scenario, the recent vigorous formation activity that took place in the bar, as well as that in the onset of the Magellanic bridge. By assuming that clusters and field stars share the same formation history, we computed the number of clusters formed per time unit using a spatially resolved SFR. We found that the cluster dissolution rate over time varies with the position in the galaxy. The Northern part of the SMC main body is pictured by

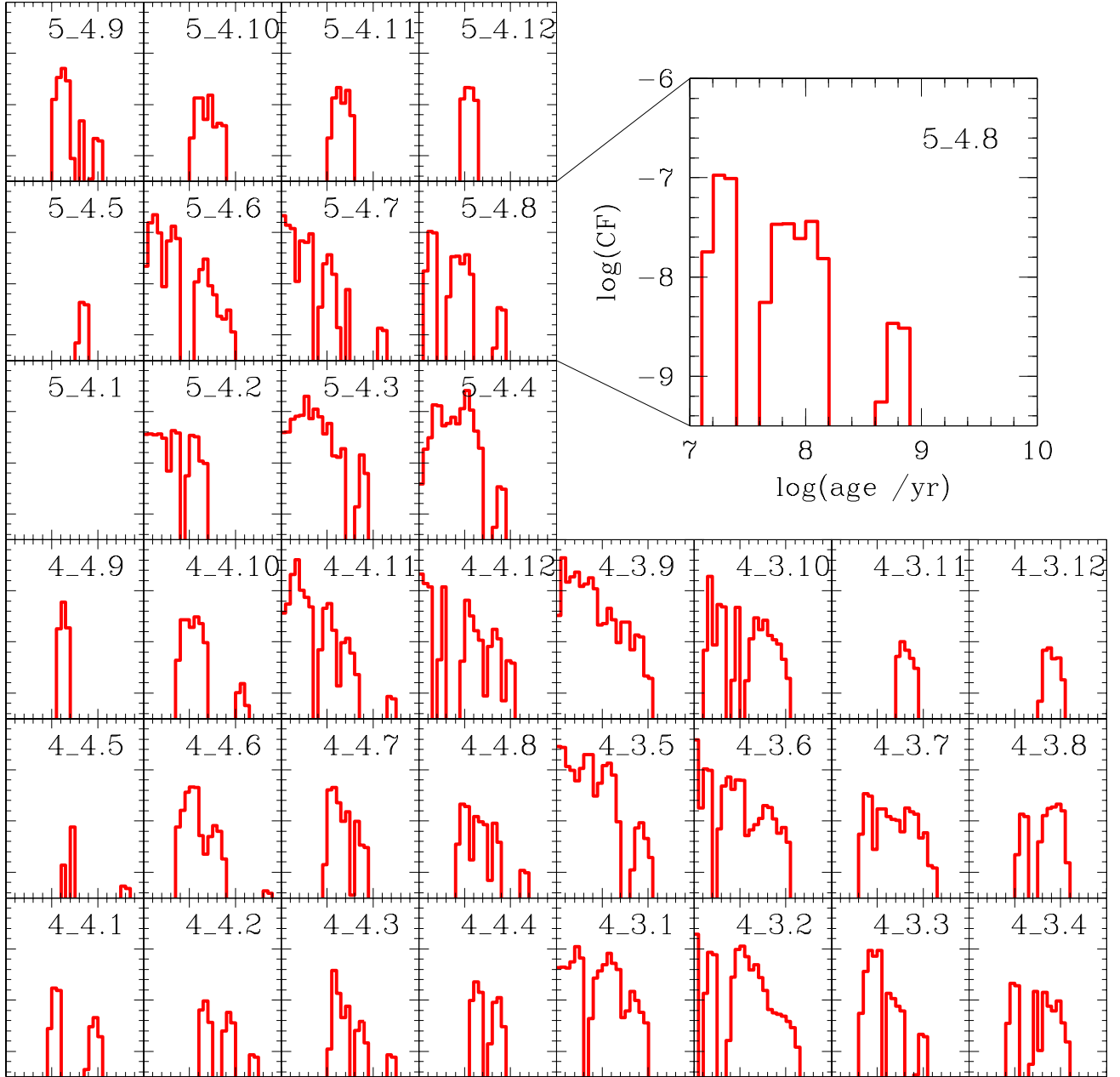


**Figure 3.** CFs for different SMC sub-fields placed following their spatial distribution pattern (see Fig. 1 and details in Section 3.1). Each panel has the same axes as illustrated in the top-right panel.

relatively small dissolution rate values in comparison with those of the SMC bar, and even those of the onset of the Magellanic bridge, where cluster disruption would seem to have been more important. We thus provide, for the first time, an observational evidence in the sense that the stronger a galactic gravitational field (e.g., larger concentration of galaxy mass, tidal forces from interaction with the LMC), the higher the cluster dissolution rate.

#### ACKNOWLEDGEMENTS

We thank the referee for the thorough reading of the manuscript and timely suggestions to improve it.

#### REFERENCES

- Baumgardt H., Parmentier G., Anders P., Grebel E. K., 2013, *MNRAS*, 430, 676  
 Besla G., Kallivayalil N., Hernquist L., van der Marel R. P., Cox T. J., Kereš D., 2012, *MNRAS*, 421, 2109

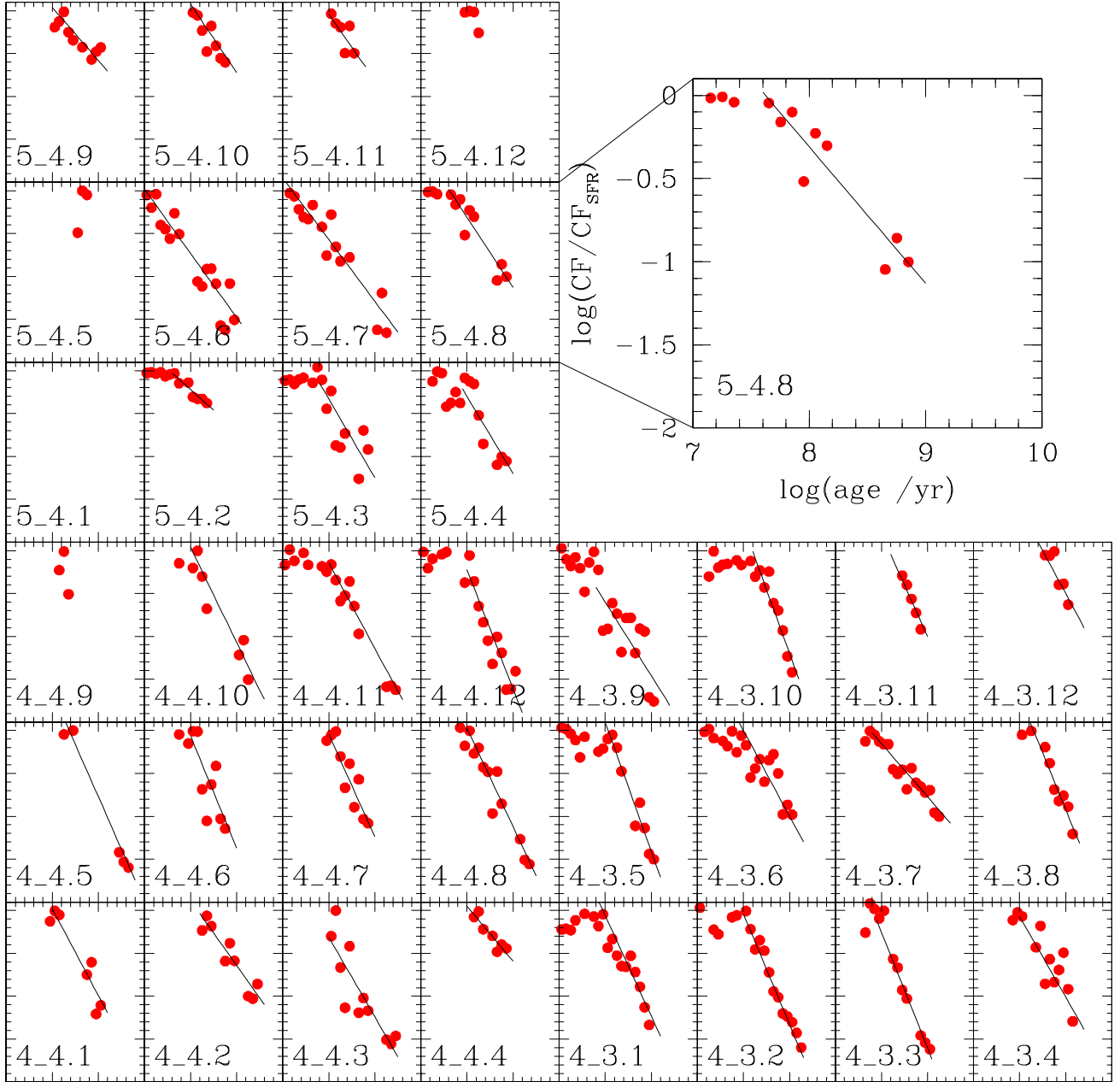


**Figure 4.** CF to  $CF_{SFR}$  ratios for different SMC fields placed following their spatial distribution pattern (see Fig. 1 and details in Section 3.1). Each panel has the same axes as illustrated in the top-right panel. The straight lines represent the fitted linear relationships (see also Table 4).

Bica E., Bonatto C., Dutra C. M., Santos J. F. C., 2008, *MNRAS*, 389, 678

Bica E., Santiago B., Bonatto C., Garcia-Dias R., Kerber L., Dias B., Barbuy B., Balbinot E., 2015, *MNRAS*, 453, 3190

Bitsakis T., González-Lópezlira R. A., Bonfimi P., Bruzual G., Maravelias G., Zaritsky D., Charlot S., Ramírez-Siordia V. H., 2018, *ApJ*, 853, 104

Carrera R., Conn B. C., Noël N. E. D., Read J. I., López Sánchez Á. R., 2017, *MNRAS*, 471, 4571

Chiosi E., Vallenari A., Held E. V., Rizzi L., Moretti A., 2006,

*A&A*, 452, 179

Cioni M.-R. L., et al., 2011, *A&A*, 527, A116

Glatt K., Grebel E. K., Koch A., 2010, *A&A*, 517, A50

Gordon K. D., et al., 2011, *AJ*, 142, 102

Harris J., Zaritsky D., 2009, *AJ*, 138, 1243

Ivanov V. D., Piatti A. E., Beamín J.-C., Minniti D., Borissova J., Kurtev R., Hempel M., Saito R. K., 2017, *A&A*, 600, A112

Mackey A. D., Koposov S. E., Da Costa G. S., Belokurov V., Erkal D., Fraternali F., McClure-Griffiths N. M., Fraser M., 2017, *MNRAS*, 472, 2975

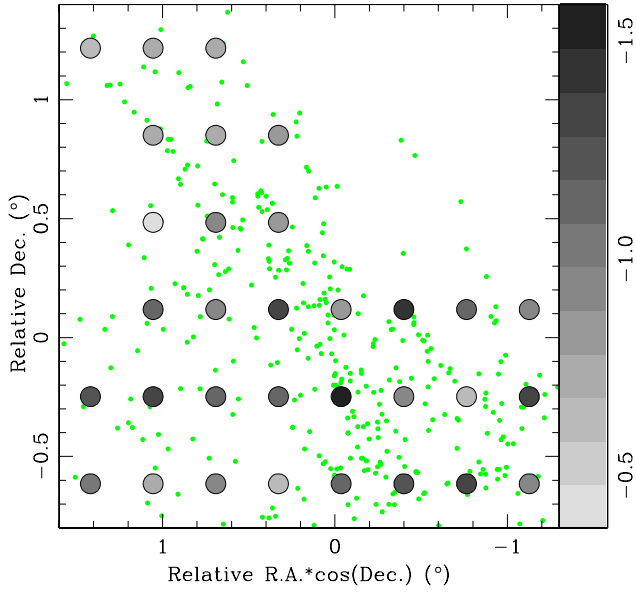


**Figure 5.** Spatial distribution of clusters in Table 2 (green dots). We superimposed the CF/CF<sub>SFR</sub> ratio slopes (Table 4) represented by grey-scale filled circles -according the colour bar- for different SMC fields.

- Maia F. F. S., Piatti A. E., Santos J. F. C., 2014, *MNRAS*, 437, 2005
- Maschberger T., Kroupa P., 2011, *MNRAS*, 411, 1495
- Noël N. E. D., Aparicio A., Gallart C., Hidalgo S. L., Costa E., Méndez R. A., 2009, *ApJ*, 705, 1260
- Noël N. E. D., Conn B. C., Read J. I., Carrera R., Dolphin A., Rix H.-W., 2015, *MNRAS*, 452, 4222
- Piatti A. E., 2011a, *MNRAS*, 416, L89
- Piatti A. E., 2011b, *MNRAS*, 418, L69
- Piatti A. E., 2014, *MNRAS*, 437, 1646
- Piatti A. E., 2017, *ApJ*, 834, L14
- Piatti A. E., Bica E., 2012, *MNRAS*, 425, 3085
- Piatti A. E., Sarajedini A., Geisler D., Clark D., Seguel J., 2007, *MNRAS*, 377, 300
- Piatti A. E., Geisler D., Sarajedini A., Gallart C., Wischnjewsky M., 2008, *MNRAS*, 389, 429
- Piatti A. E., de Grijs R., Rubele S., Cioni M.-R. L., Ripepi V., Kerber L., 2015, *MNRAS*, 450, 552
- Piatti A. E., Ivanov V. D., Rubele S., Marconi M., Ripepi V., Cioni M.-R. L., Oliveira J. M., Bekki K., 2016, *MNRAS*, 460, 383
- Pietrzynski G., Udalski A., Kubiak M., Szymanski M., Wozniak P., Zebrun K., 1998, *Acta Astron.*, 48, 175
- Piskunov A. E., Just A., Kharchenko N. V., Berczik P., Scholz R.-D., Reffert S., Yen S. X., 2018, preprint, ([arXiv:1802.06779](https://arxiv.org/abs/1802.06779))
- Rubele S., et al., 2015, *MNRAS*, 449, 639
- Sabbi E., et al., 2009, *ApJ*, 703, 721
- Shapley H., Wilson H. H., 1925, *Harvard College Observatory Circular*, 276, 1
- Siegel M. H., et al., 2014, *AJ*, 148, 131
- Simons R., Thilker D., Bianchi L., Wyder T., 2014, *Advances in Space Research*, 53, 939
- Skowron D. M., et al., 2014, *ApJ*, 795, 108
- Weisz D. R., Dolphin A. E., Skillman E. D., Holtzman J., Dalcanton J. J., Cole A. A., Neary K., 2013, *MNRAS*, 431, 364
- Yozin C., Bekki K., 2014, *MNRAS*, 443, 522

Zaritsky D., Harris J., Thompson I. B., Grebel E. K., Massey P., 2002, *AJ*, 123, 855

van der Marel R. P., Kallivayalil N., 2014, *ApJ*, 781, 121

This paper has been typeset from a  $\text{\TeX}/\text{\LaTeX}$  file prepared by the author.